

## Supplementary Data

### Isolation of acute myeloid leukemia blasts from blood using a microfluidic device

Alexandra Teixeira<sup>a, b, c</sup>, Maria Sousa-Silva<sup>a, d</sup>, Alexandre Chícharo<sup>a</sup>, Kevin Oliveira<sup>a</sup>, André Moura<sup>e</sup>, Adriana Carneiro<sup>a, f, g</sup>, Paulina Piairo<sup>a</sup>, Hugo Águas<sup>e</sup>, Belém Sampaio-Marques<sup>b, c</sup>, Isabel Castro<sup>b, c</sup>, José Mariz<sup>h</sup>, Paula Ludovico<sup>b, c</sup>, Sara Abalde-Cela<sup>a</sup> and Lorena Diéguez<sup>a\*</sup>

<sup>a</sup>. *International Iberian Nanotechnology Laboratory (INL), Avda. Mestre José Veiga, 4715-310 Braga, Portugal*

<sup>b</sup>. *Life and Health Sciences Research Institute (ICVS), Escola de Medicina, Universidade do Minho, Campus Gualtar, 4710-057 Braga, Portugal*

<sup>c</sup>. *ICVS/3B's - PT Government Associate Laboratory, Braga/Guimarães, Portugal*

<sup>d</sup>. *RUBYNanomed LDA, Praça Conde de Agrolongo, 4700-312 Braga, Portugal*

<sup>e</sup>. *CENIMAT/i3N, Materials Science Department, Faculdade de Ciência e Tecnologia—Universidade Nova de Lisboa, 2829-516 Lisbon, Portugal*

<sup>f</sup>. *IPO Experimental Pathology and Therapeutics Group, Research Center of IPO Porto (CI-IPOP)/RISE@CI-IPOP (Health Research Network), Portuguese Oncology Institute of Porto (IPO Porto), Porto Comprehensive Cancer Center (Porto.CCC), 4200-072 Porto, Portugal.*

<sup>g</sup>. *Instituto de Ciências Biomédicas Abel Salazar (ICBAS), Universidade do Porto, Porto, Portugal*

<sup>h</sup>. *Department of Oncohematology, Portuguese Institute of Oncology Francisco Gentil Porto, Portugal*

## Supplementary Figures

Videos of simulations (Images of the videos to send)

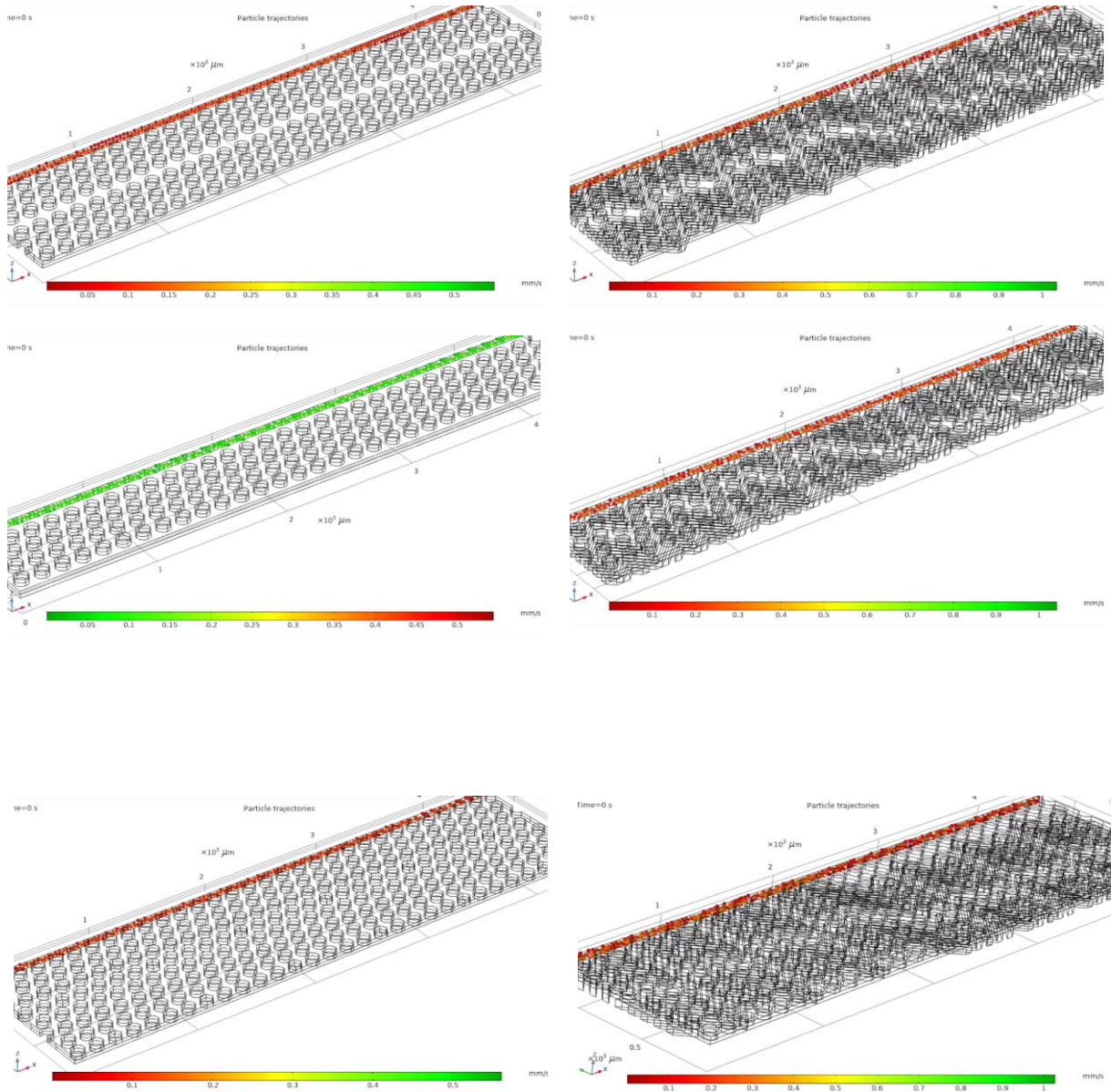
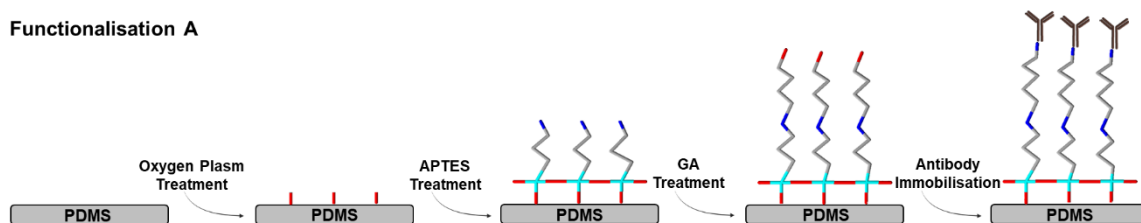


Figure S1: Images from the videos obtained in the simulations. In the left, from the top to the bottom, is represented a section of each type of design: 3 lines, 4 lines and full lines, respectively. These sections were subjected to simulations in order to access to theoretical information about which design and geometry can potentially display a higher capture efficiency. In the right side the same pillar devices combined with the herringbones.

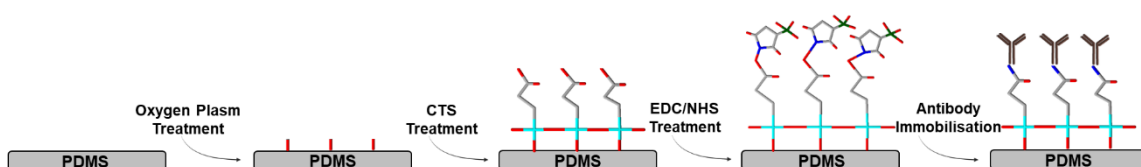
**Table S1:** Results of the simulations in a section of the device and then extrapolated for whole devices.

# particles stuck in unit cell		3L	3L + HB	4L	4L + HB	FL	FL + HB
	2 $\mu\text{L}/\text{min}$	66	71	71	61	108	93
	20 $\mu\text{L}/\text{min}$	60	68	69	61	113	90
	40 $\mu\text{L}/\text{min}$	62	70	68	60	110	100
% particles stuck in unit cell	300	3L	3L + HB	4L	4L + HB	FL	FL + HB
	2 $\mu\text{L}/\text{min}$	22.00%	23.67%	23.67%	20.33%	36.00%	31.00%
	20 $\mu\text{L}/\text{min}$	20.00%	22.67%	23.00%	20.33%	37.67%	30.00%
	40 $\mu\text{L}/\text{min}$	20.67%	23.33%	22.67%	20.00%	36.67%	33.33%
% particles stuck in whole chip, according # unit cells	300	3L	3L + HB	4L	4L + HB	FL	FL + HB
	2 $\mu\text{L}/\text{min}$	93.50%	94.87%	97.72%	95.85%	98.20%	96.45%
	20 $\mu\text{L}/\text{min}$	91.41%	94.08%	97.42%	95.85%	98.58%	95.96%
	40 $\mu\text{L}/\text{min}$	92.17%	94.62%	97.26%	95.60%	98.36%	97.40%

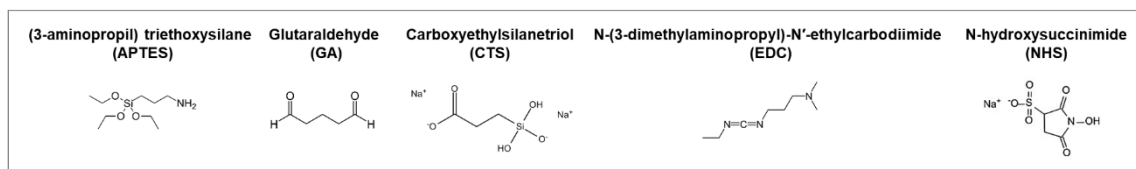
### Functionalisation A



### Functionalisation B



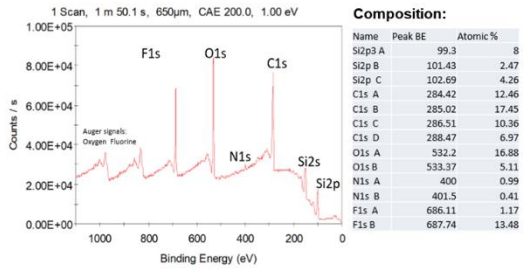
● OH   ● Si   ● CH<sub>3</sub>   ● NH   ● S



*Scheme S1. Schematic representation of the two different functionalisation strategies. Both characterised by the preliminar treatment with oxygen plasma to covalently bind functional silanes. Functionalisation A anchors the antibody through APTES and Glutaraldehyde (top); while functionalisation B composed links the antibody through CTS, activated with EDC/NHS (bottom).*

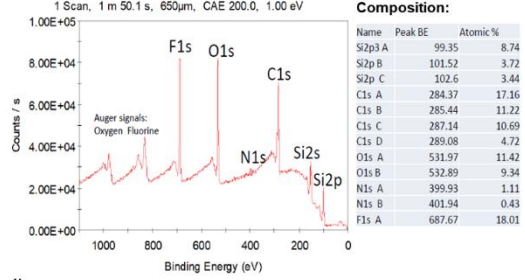
A

i

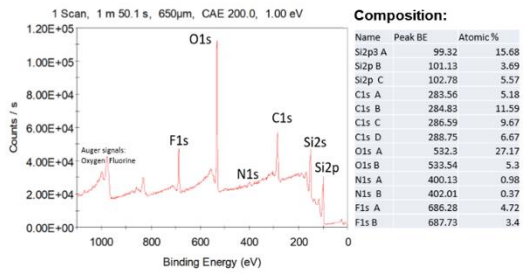


B

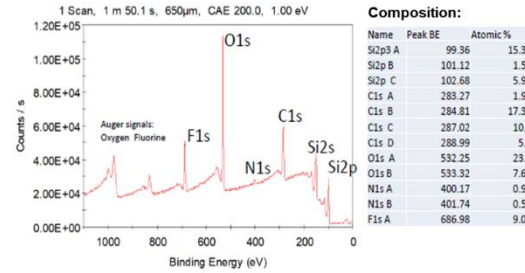
i



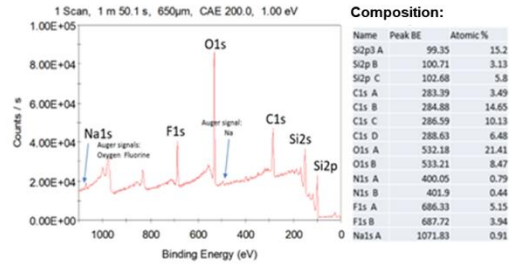
ii



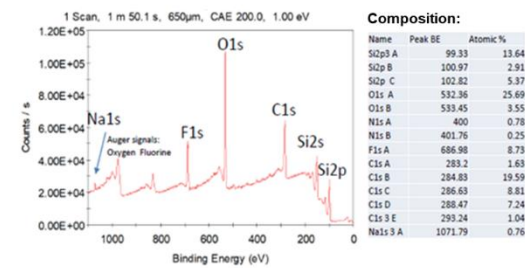
ii



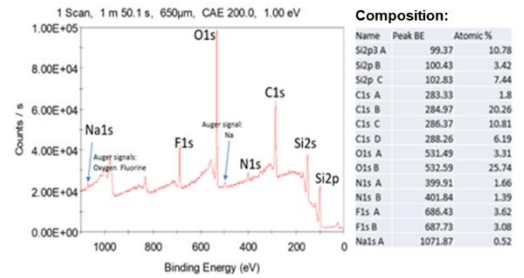
iii



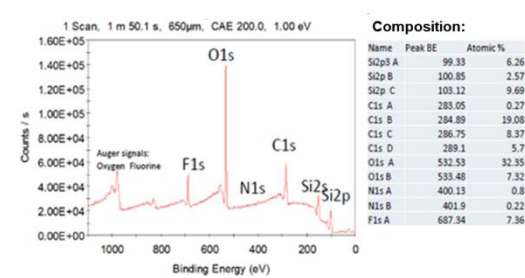
iii



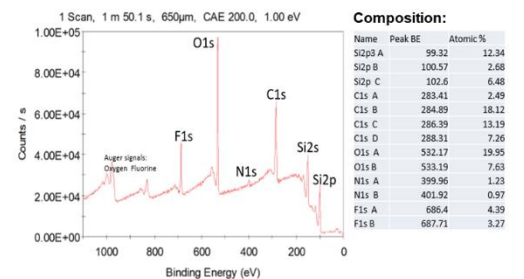
iv



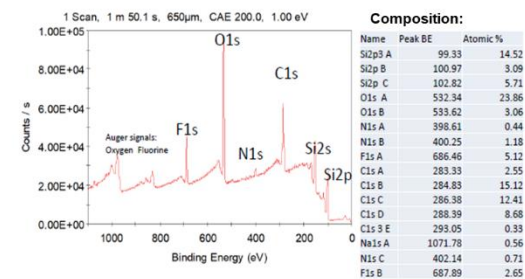
iv



v



v



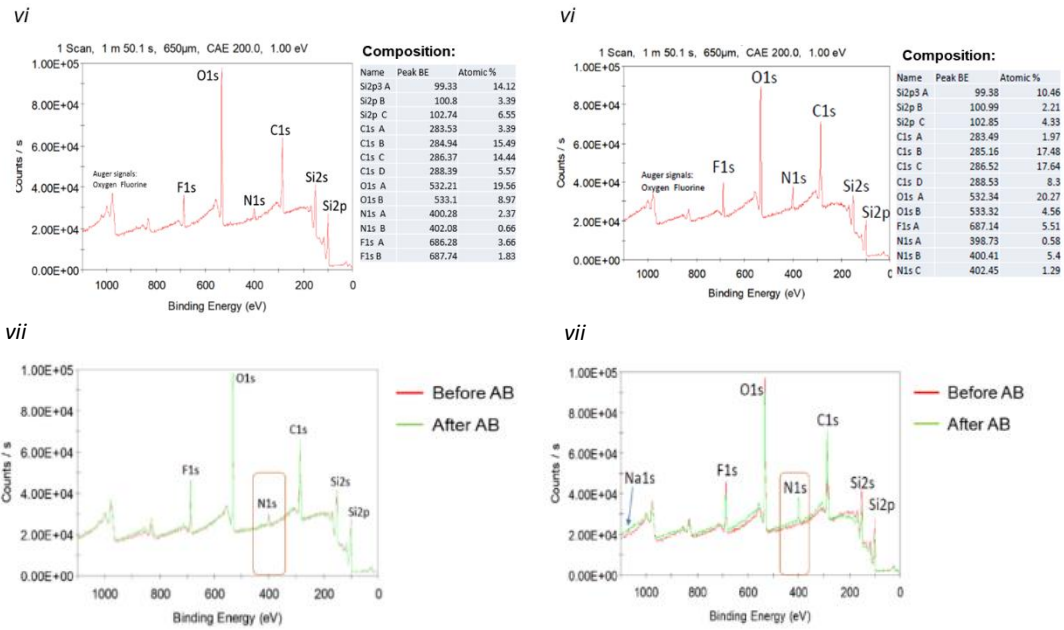


Figure S2: XPS results of the silicon wafer treated with the two different functionalisation protocols. Functionalisation A based in the application of APTES, Glutaraldehyde and antibody (A) and Functionalisation B consists in the utilisation of CTS, EDC/NHS and antibody (B). XPS analysis was performed at each of the steps of the functionalisation protocol: silicon wafer before all the process (A i and B i); after plasma cleaner (A ii and B ii); after ethanol (A iii and B iii); after silane APTES (A iv) and CTS (B iv); after Glutaraldehyde (A v) and after EDC/NHS (B v); antibody (A vi and B vi). Comparison before and after the incubation of the antibody (A vii and B vii).

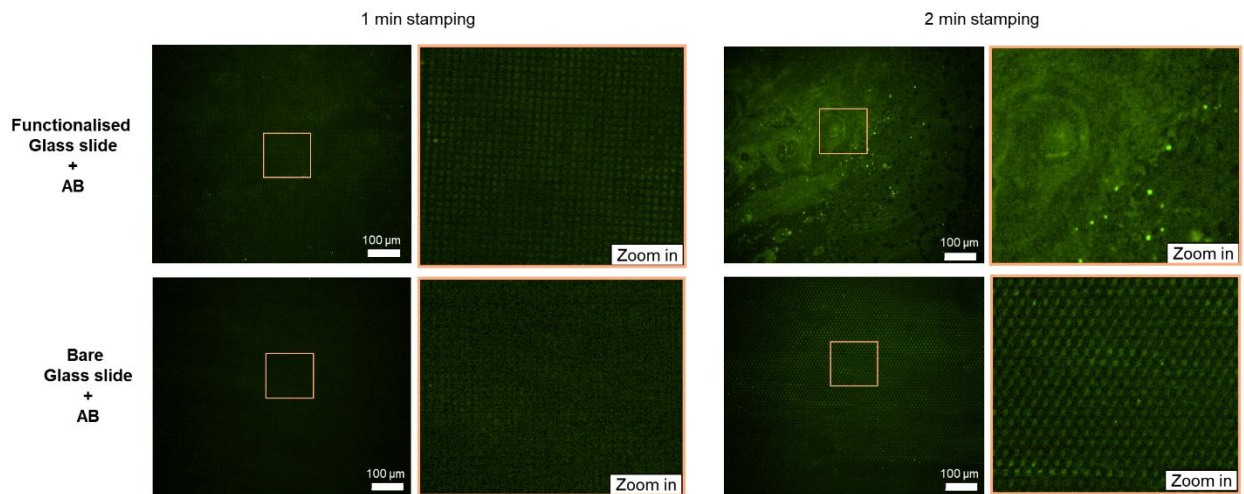


Figure S3: Fluorescently labelled antibody (in green) are patterned onto functionalised and bare glass slides by microcontact printing using a PDMS stamp.

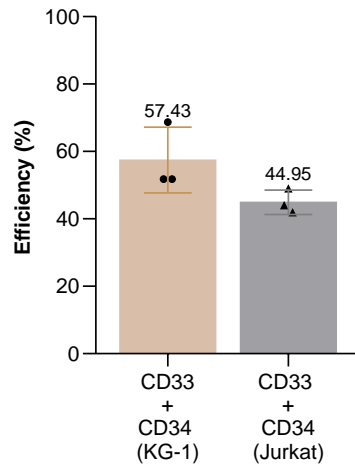


Figure S4: Capture efficiency (%) of target cells in devices with CD33 and CD34 antibodies immobilised on the surface, using pillars (gap every 4 lines) combined with herringbone, using a flow rate of 40  $\mu\text{L}/\text{min}$ . The results are presented as mean  $\pm$  SD of 3 independent biological replicates. Student's t test was applied to compare KG-1 (CD33+ / CD34+) and Jurkat (CD33- / CD34-) cells isolation efficiency. \* $p < 0.05$ .

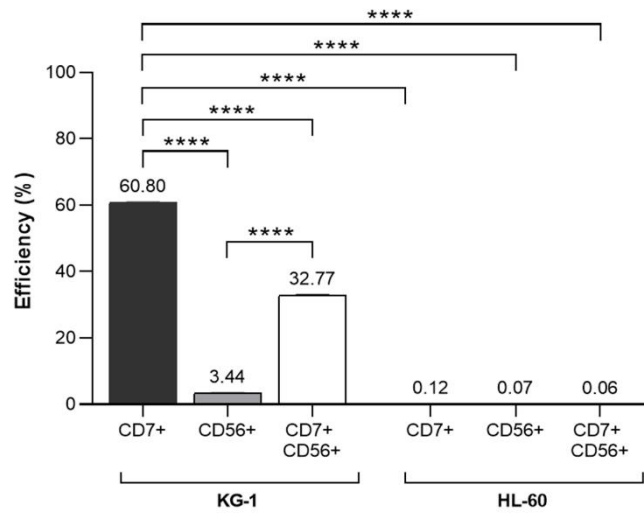
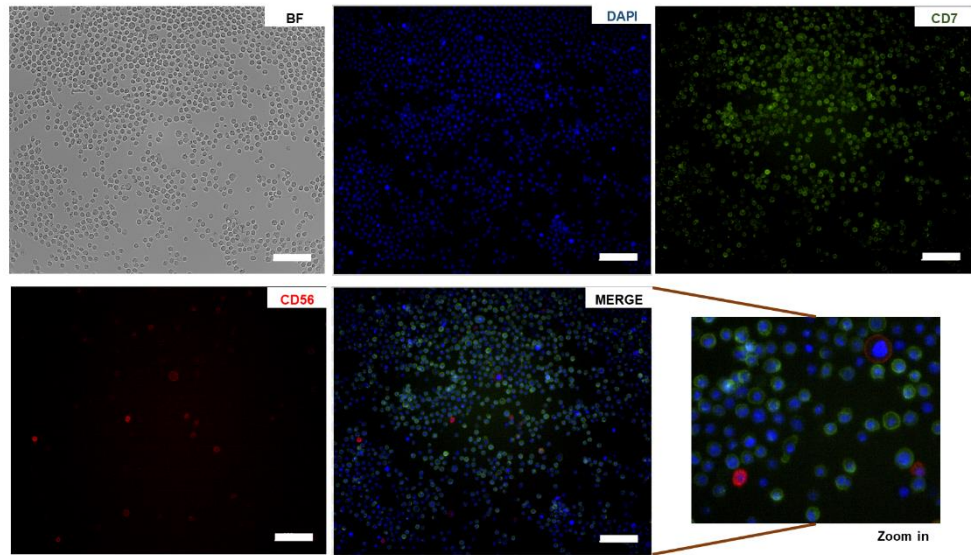
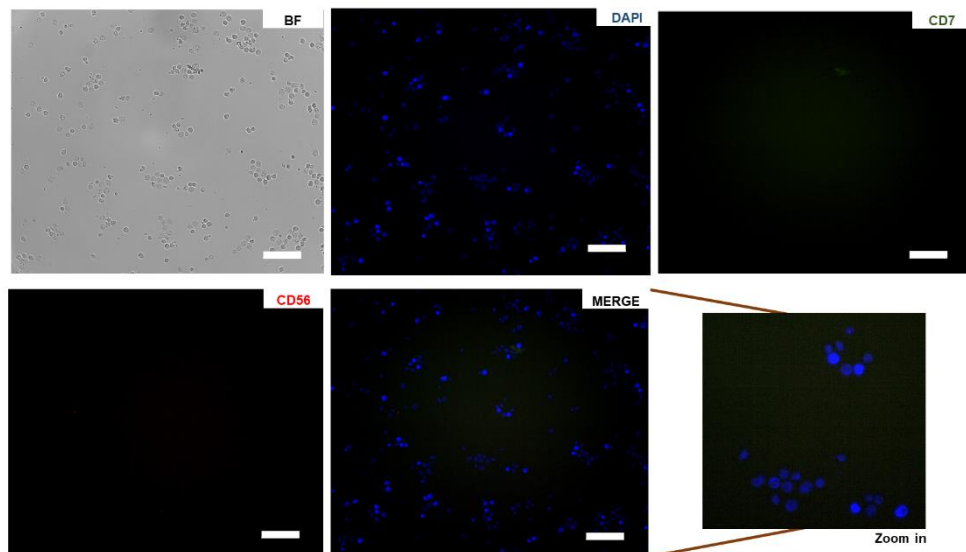
**A****B***i**ii*

Figure S5. FC analysis and microscopic images obtained from immunocytochemistry (ICC) assays, in well-plates, for aberrant surface markers in AML cells. CD34 positivity was significantly different and higher in the KG-1 cells (A). Phenotypical characterization using CD7 and CD56 markers in AML cells (B): KG-1 and (i) HL-60 (ii) cells seeded in a well-plate. All cells were stained for DAPI (1:10), and CD7 and CD56 (1:50), in blue, green and red, respectively.

The FC results presented as mean  $\pm$  SD of 3 independent biological replicates. For the flow rates and controls an one-way ANOVA and Tukey's post hoc test were used to compare the different flow rates in the same type of device (gap every 4 lines), as well as for the different controls using the same device and flow rate. For the analysis of FC results a 2 way ANOVA test was applied to compare the expression of CD7, CD56 and both in KG-1 and HL-60 cells. \*\*\*\* $p < 0.0001$ .

Table S2. Table with NGS results from clinical samples. Genetic analysis of the samples through a panel selected for the study of AML patients. Multiple genes relevant to AML disease were considered, as well as genes not associated with AML, but potential targets for study in this disease

Sample	Gene	Variant allele frequency (VAF %)		c.DNA	Protein	Classification	Observations
		BM	PB				
Patient 1	FLT3	>5	>5	c.1773_1793dup	p.(Tyr597_Glu598ins AspValAspPheArgGluTyr)	TIER I	Prognostic and therapeutic indication in AML
	IDH2	>5	>5	c.419G>A	p.(Arg140Gln)	TIER I	Prognostic and therapeutic indication in AML
	NPM1	>5	>5	c.860_863dup	p.(Trp288Cysfs*12)	TIER I	Prognostic and therapeutic indication in AML
	ETV6	>5	>5	c.602T>C	p.(Leu201Pro)	TIER III	Not associated with AML
	SRSF2	>5	>5	c.284C>G	p.(Pro95Arg)	TIER I	Associated with AML
	SETBP1	>5	>5	c.691G>C	p.(Val231Leu)	TIER IV	Without clinical significance
	TET2	>5	>5	c.5162T>G	p.(Leu1721Trp)	TIER IV	Without clinical significance
	ASXL1	>5	>5	c.2444T>C	p.(Leu815Pro)	TIER IV	Without clinical significance
	KIT	>5	>5	c.1621A>C	p.(Met541Leu)	TIER III	Associated with AML
	TP53	>5	>5	c.215C>G	p.(Pro72Arg)	TIER IV	Without clinical significance
Patient 2	TP53	>5	>5	c.375+5G>	unknown	TIER III	Not associated with AML
	TP53	>5	>5	c.215C>G	p.(Pro72Arg)	TIER IV	Without clinical significance
	CSF3R	>5	>5	c.1319G>A	p.(Arg440Gln)	TIER IV	Without clinical significance
	SETBP1	>5	>5	c.3388C>A	p.(Pro1130Thr)	TIER III	Not associated with AML
	TET2	>5	>5	c.1064G>A	p.(Gly355Asp)	TIER IV	Without clinical significance
	TET2	>5	>5	c.5284A>G	p.(Ile1762Val)	TIER IV	Without clinical significance
	ASXL1	>5	>5	c.5284A>G	p.(Leu815Pro)	TIER IV	Without clinical significance